

Two-Photon Correlations in X-rays from a Synchrotron Radiation Source

Yorinobu Kunimune,^{a†} Yoshitaka Yoda,^a Koichi Izumi,^{a‡} Makina Yabashi,^a Xiao-Wei Zhang,^b Taikan Harami,^c Masami Ando^b and Seishi Kikuta^a

^aDepartment of Applied Physics, School of Engineering, University of Tokyo, 7-3-1 Hongo, Bunkyo-ku, Tokyo 113, Japan, ^bPhoton Factory, National Laboratory for High Energy Physics, 1-1 Oho, Tsukuba-shi, Ibaraki 305, Japan, and ^cSynchrotron Radiation Facility Laboratory, Japan Atomic Energy Research Institute, Harima Science Garden City, Kamigori-cho, Akoh-gun, Hyogo 278-12, Japan. E-mail: kikuta@kohsai.t.u-tokyo.ac.jp

(Received 12 December 1996; accepted 6 May 1997)

The intensity correlation experiment using visible light performed by Hanbury Brown & Twiss [*Nature (London)* (1956), **177**, 27–29] is extended to X-ray wavelengths. Correlations of 14.4 keV X-ray photons from a synchrotron radiation source are observed by the coincidence counting technique. The high brilliance of synchrotron radiation available in the Tristan main ring enables the observation of two-photon correlations with a reasonable measurement time.

Keywords: X-ray two-photon correlations; Hanbury Brown–Twiss experiment; bunching effect of photons; X-ray coherence.

1. Introduction

The intensity correlation experiment using visible light was first demonstrated by Hanbury Brown & Twiss (1956a). They observed that photons in a monochromatic light beam from a thermal source did not arrive completely at random but arrived in bunches. This technique was further applied to an optical stellar intensity interferometer and the angular diameter of visible stars was determined (Hanbury Brown & Twiss, 1956b). About 20 years after their pioneering work the observation of two-photon correlations with synchrotron radiation was proposed (Shuryak, 1975). The difference in the visible photon counting statistics between synchrotron radiation from a wiggler and that from a bending magnet has actually been observed (Tanabe, Teich & Marshall, 1991). However, for the observation of such a phenomenon for X-rays one had to wait for the realization of high-brilliance synchrotron radiation sources. This is because the temporal and spatial coherence conditions in the X-ray region are much more severe to fulfill than those in the visible light region. This experiment may be applied to the determination of the transverse synchrotron radiation source size of third-generation rings which is approaching the diffraction limit. Intensity correlation experiments are planned for such purposes at third-generation synchrotron radiation facilities (Ikonen, 1992; Gluskin, McNulty, Vicarro & Howells, 1992).

† Present address: ULSI Device Development Laboratory, NEC, 1120 Shimokuzawa, Sagami-hara, Kanagawa 229, Japan.

‡ Present address: Fundamental Research Laboratory, NEC, 34 Miyuki-gaoka, Tsukuba-shi, Ibaraki 305, Japan.

Hanbury Brown & Twiss (1956a) used analog detectors of current-mode type and observed the correlation of the fluctuating output currents from two detectors. On the other hand, in the present experiment a photon counting technique was adopted in which the coincidence rate between pulses from two detectors was observed. To normalize the coincidence rate a unique method was attempted which uses, in addition to a synchrotron radiation pulse from a certain electron bunch, a synchrotron radiation pulse from the same electron bunch after a further revolution of the ring. The coincidence rate is expected to become higher than the random coincidence rate when the intensities are correlated.

2. Second-order degree of coherence

The theoretical background of the correlation in a radiation field is described. The usual interference experiments are related to the correlation of radiation field amplitudes. The first-order degree of coherence, $\gamma_{12}^{(1)}(\tau)$, represents the correlation between the field at position \mathbf{r}_1 and time t_1 and the complex conjugate field at \mathbf{r}_2 and t_2 . It is time-dependent, since $\tau = t_1 - t_2$. Under the condition of cross-spectral purity $\gamma_{12}^{(1)}(\tau)$ is expressed as a product of two factors, *i.e.*

$$\gamma_{12}^{(1)}(\tau) = \gamma_{12}^{(1)}(0)\gamma_{11}^{(1)}(\tau). \quad (1)$$

On the other hand, the intensity correlation caused by interference of two photons is expressed in terms of the second-order degree of coherence given by

$$\gamma_{12}^{(2)}(\tau) = \frac{\langle I(\mathbf{r}_1, t) I(\mathbf{r}_2, t + \tau) \rangle}{\langle I(\mathbf{r}_1, t) \rangle \langle I(\mathbf{r}_2, t) \rangle}. \quad (2)$$

Here, $I(\mathbf{r}, t)$ is the intensity at position \mathbf{r} and time t . $\langle \dots \rangle$ denotes the time average. For thermal light $\gamma_{12}^{(2)}(\tau)$ is expressed as

$$\gamma_{12}^{(2)}(\tau) = 1 + |\gamma_{12}^{(1)}(\tau)|^2. \quad (3)$$

In (3) the second-order degree of coherence becomes 2 when $\tau = 0$. This shows the bunching effect of photons. This effect is blurred with the incomplete spatial and temporal coherence. Using (1), (3) becomes

$$\gamma_{12}^{(2)}(\tau) = 1 + |\gamma_{12}^{(1)}(0)|^2 |\gamma_{11}^{(1)}(\tau)|^2. \quad (4)$$

When the pulse width of synchrotron radiation is longer than the longitudinal coherence length of the beam, the intensity correlation is weakened. Similarly, when the cross section of the beam is larger than the transverse coherence area, the intensity correlation is also weakened. Taking account of the synchrotron radiation pulse width and the beam cross section, the integrated second-order degree of coherence becomes

$$\begin{aligned} \gamma^{(2)} &= d_x^{-2} d_y^{-2} \int_{-d_x/2}^{d_x/2} dx_1 \int_{-d_y/2}^{d_y/2} dy_1 \int_{-d_x/2}^{d_x/2} dx_2 \int_{-d_y/2}^{d_y/2} dy_2 \\ &\times \tau_p^{-2} \int_{-\tau_p/2}^{\tau_p/2} dt_1 \int_{-\tau_p/2}^{\tau_p/2} dt_2 \gamma_{12}^{(2)}(\tau) \\ &= 1 + F(\pi^{1/2} d_x / l_x) F(\pi^{1/2} d_y / l_y) \tau_c / \tau_p. \end{aligned} \quad (5)$$

Here,

$$F(b) = (2/b) \int_0^b e^{-u^2} du - (1 - e^{-b^2})/b^2, \quad (6)$$

$$l_x = \lambda D / 2\pi^{1/2} \sigma_x, \quad l_y = \lambda D / 2\pi^{1/2} \sigma_y. \quad (7)$$

l_x and l_y are the transverse coherence widths in the horizontal and vertical directions, d_x and d_y are the horizontal and vertical slit widths, σ_x and σ_y are the standard deviations of the Gaussian source size, λ is the wavelength, D is the distance between source and detector, τ_c is the coherence time of the beam and τ_p is the pulse width of synchrotron radiation. It is assumed that τ_p is much larger than τ_c . $\gamma^{(2)}$ is expressed more simply by replacing the second term of

(3) with $1/M$ (Goodman, 1985), i.e.

$$\gamma^{(2)} = 1 + 1/M, \quad (8)$$

where M is the number of coherence cells which always takes a value greater than unity.

3. Experiment

The experiment was carried out at a test synchrotron radiation beamline temporarily constructed in the Tristan main ring at the National Laboratory for High Energy Physics, Japan. An in-vacuum-type X-ray undulator was installed (Yamamoto, Sugiyama, Tsuchiya & Shioya, 1997). The Tristan main ring was operated at an energy of 10 GeV in the eight-bunch mode. The ring current was kept between 9 and 5 mA during the experiment. The brilliance of synchrotron radiation from the undulator was about 10^{18} photons s^{-1} mm^{-2} $mrad^{-2}$ (0.1% bandwidth) $^{-1}$ and of the same order of magnitude as those in third-generation synchrotron radiation sources. The experimental parameters of our analysis are listed in Table 1, and the experimental set-up is shown in Fig. 1. X-rays from the undulator were roughly monochromatized at 14.4 keV by an Si(400) double-crystal monochromator. Next, a high-energy-resolution four-crystal Si monochromator was set up, composed of two channel-cut Si crystals nested with each other, in which 422 asymmetric reflections were served as the first and fourth reflection and 12 2 2 symmetric reflections were served as the second and third reflection. Highly monochromatic X-rays with an energy width of 6.4 meV were obtained. This energy width determined the temporal coherence of the X-ray beam. The coherence time, τ_c , was estimated to be 0.66 ps. The optimum condition for the coherence time is that it almost equals the synchrotron radiation pulse width, τ_p . In this experiment the energy width of the X-rays corresponding to the optimum coherence time was 10 μ eV. Since a monochromator with about 10 μ eV energy width was not realizable, the above-mentioned monochromator was used although it did not provide satisfactory conditions.

After the four-crystal Si monochromator a precise slit was arranged, which determined the spatial coherence of the beam. The intensity distribution of the source was assumed to be Gaussian. The nominal source sizes in the horizontal and vertical directions were $\sigma_x \simeq 169$ μ m and $\sigma_y \simeq 53$ μ m.

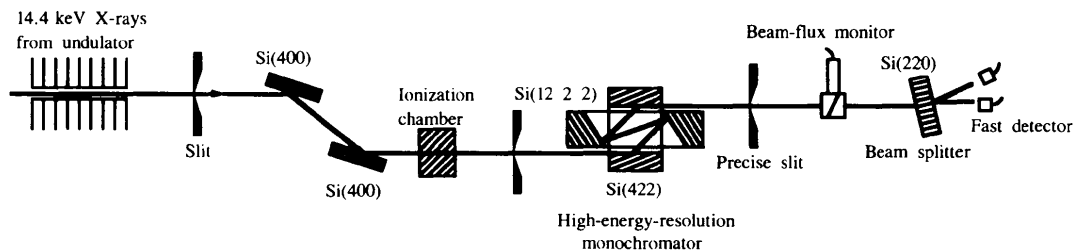


Figure 1
Schematic side-view of the experimental set-up.

Table 1
Experimental parameters.

Wavelength	λ	0.086 nm
Distance between source and detector	D	~ 100 m
Pulse width of synchrotron radiation	τ_p	~ 60 ps
Pulse interval of synchrotron radiation (eight-bunch mode)	ΔT	1.25 μ s
Horizontal source size	σ_x	~ 169 μ m
Vertical source size	σ_y	~ 53 μ m
Horizontal coherence width	l_x	~ 14 μ m
Vertical coherence width	l_y	~ 46 μ m

The transverse coherence widths of X-rays in the horizontal and vertical directions at a detector position located at $D \simeq 100$ m from the synchrotron radiation source were calculated as $l_x \simeq 14$ μ m and $l_y \simeq 46$ μ m, using (7). The optimum condition for the slit size is that it is almost the same as the transverse coherence width. The vertical slit width was fixed at 40 μ m, while the horizontal slit width was varied from 20 μ m to 1 mm. The blades of slits made of tantalum metal were driven by stepping motors and their positions were read by linear encoders. The slit width was set to an accuracy of 1 μ m.

The Si 220 Laue case diffraction served as the beam splitter. The thickness of the crystal plate was 4 mm. The diffracted and transmitted beams were incident on avalanche photodiode detectors. The beam splitter was necessary to make coincidence measurements since the time resolution of the detector was longer than the pulse width of the synchrotron radiation. Now consider the case where two photons relevant to the measurement are included in a synchrotron radiation pulse. Only when two photons in the same pulse are separated from each other by the splitter is a coincidence event counted. If both photons are diffracted or transmitted in the splitter, then no coincidence event is counted.

4. Principle of measurements

A block diagram of the photon-counting system is shown in Fig. 2. Output pulses from two detectors were fed into the coincidence unit and then scaler 1 counted the number of coincidences. In the delay circuit the delay time for the output pulse from one detector was set at the circulation period of electrons, 10 μ s. Random coincidence events

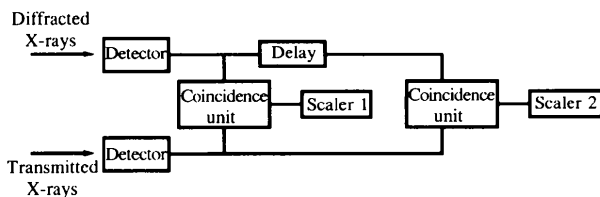


Figure 2
Block diagram of the photon-counting system. Three sets of a delay circuit, a coincidence unit and a scaler were additionally connected in series.

between one photon emitted from a certain electron bunch and another photon emitted from the same electron bunch after making one revolution were counted at scaler 2. It is essential to use the same electron bunch because each bunch has a different number of electrons. These coincidence measurement events are illustrated in Fig. 3. Coincidence counts measured at scalers 1 and 2 were denoted by R and R_0 , respectively. R was normalized by using R_0 . To reduce statistical uncertainty of the random coincidence rate it was counted between two photons separated at intervals of 20, 30 and 40 μ s, as well as at 10 μ s.

In this experiment we assume that synchrotron radiation can be treated in the same way as thermal light. The probability distribution for K photoelectric counts in a pulse is given by (Goodman, 1985)

$$P(K) = \frac{\Gamma(K+M)}{\Gamma(K+1)\Gamma(M)} \left(1 + \frac{\bar{K}}{M}\right)^{-M} \left(1 + \frac{M}{\bar{K}}\right)^{-K}, \quad (9)$$

where \bar{K} is the average number of counts in a pulse and M is the number of coherence cells defined in (8). The total coincidence count, R , and random coincidence count, R_0 , in a measurement time, T , are given by

$$R = \sum_{K=2}^{\infty} P(K) \left[1 - r^K - (1-r)^K\right] T/\Delta T, \quad (10)$$

$$R_0 = \left[\sum_{K=1}^{\infty} P(K)(1-r^K) \right] \left\{ \sum_{K=1}^{\infty} P(K) \left[1 - (1-r)^K\right] \right\} T/\Delta T, \quad (11)$$

where r is the ratio of beam splitting and ΔT is the pulse interval. By referring to the probability generating function of the negative binomial distribution as

$$\sum_{K=0}^{\infty} P(K)r^K = \left\{ M / \left[M + (1-r)\bar{K} \right] \right\}^M, \quad (12)$$

the ratio R/R_0 is approximately given by

$$R/R_0 = 1 + 1/M - \bar{K}/2M. \quad (13)$$

In (13) the terms above the first power \bar{K}/M are neglected since $\bar{K}/2M \ll 1$. On substituting (8) into (13) one obtains

$$R/R_0 = \gamma^{(2)} - \bar{K}/2M. \quad (14)$$

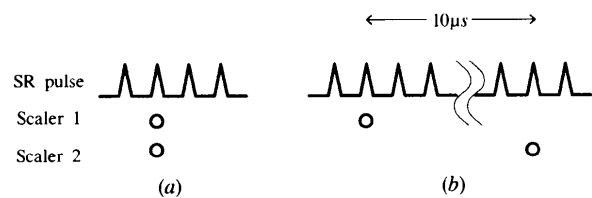


Figure 3
Representation of (a) a coincidence event and (b) a random coincidence event. The random coincidence events are counted when two photons arrive at intervals of 10, 20, 30 and 40 μ s.

As shown later, the term $\bar{K}/2M$ in (14) can be neglected in the present experimental condition. Then (14) becomes

$$R/R_0 = \gamma^{(2)}. \quad (15)$$

This shows that normalization of R by R_0 gives $\gamma^{(2)}$. Using this method we can expect to measure $\gamma^{(2)}$ to a high accuracy.

5. Results and discussion

As shown in Table 2, total coincidence counts, R , and random coincidence counts, R_0 , were measured for measurement times, T , at five horizontal slit widths, and the values of the integrated second-order degree of coherence, $\gamma^{(2)}$, were obtained as the ratio R/R_0 . Here, R_0 is an averaged value of four random coincidence counts measured between two photons separated at intervals of 10, 20, 30 and 40 μs .

To show that the approximation made in (15) is reasonable, comparisons of magnitude are made between $\bar{K}/2M$ and the statistical error, σ_γ , of $\gamma^{(2)}$, as shown in Table 3. It is evident that $\bar{K}/2M$ is much smaller than σ_γ . Therefore one can neglect the term $\bar{K}/2M$.

Fig. 4 shows the variation of the integrated second-order degree of coherence, $\gamma^{(2)}$, as a function of horizontal slit width. The experimental results are plotted as points with their associated statistical errors. The full line is the theoretical curve, which was calculated by using the nominal source sizes listed in Table 1. The dotted straight line, $\gamma^{(2)} = 1$, shows the random coincidence level. The region above this level is considered as the contribution from the excess coincidence rate. At a slit size of 20 $\mu\text{m} \times 40 \mu\text{m}$ the excess part is about four times as large as the associated statistical error. As the slit size increases, the value of $\gamma^{(2)}$ decreases, approaching unity. At a slit size of 1 mm \times 40 μm , $\gamma^{(2)}$ is very close to unity. The data and expected curves agree relatively well, giving clear evidence for the bunching effect of X-ray photons.

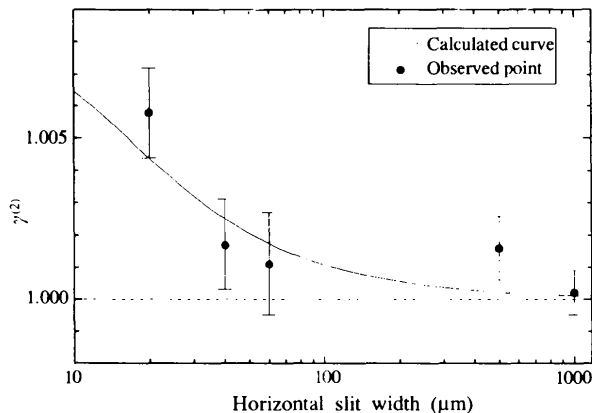


Figure 4

Variation of the integrated second-order degree of coherence, $\gamma^{(2)}$, with the horizontal slit width. The error bars show the statistical errors.

Table 2

Observed results of coincidence counts.

T is the measurement time, R is the total coincidence count and R_0 is the random coincidence count.

Slit size (μm)	T (s)	R	R_0	R/R_0
20 \times 40	43770	669556	665709	1.0058
40 \times 40	12720	624067	622993	1.0017
60 \times 40	8310	469205	468682	1.0011
500 \times 40	650	1213796	1212017	1.0015
1000 \times 40	1090	2967164	2956702	1.0002

Table 3

Comparison between observed $\bar{K}/2M$ and the statistical error, σ_γ , of $\gamma^{(2)}$.

Slit size (μm)	\bar{K}	$\bar{K}/2M$	σ_γ
20 \times 40	0.007	0.00002	0.0014
40 \times 40	0.014	0.00001	0.0014
60 \times 40	0.014	0.00001	0.0016
500 \times 40	0.144	0.00011	0.0010
1000 \times 40	0.141	0.00001	0.0007

When we calculated the theoretical value of $\gamma^{(2)}$ we treated synchrotron radiation as thermal light. Considering the agreement between experiment and theory, we can say that this assumption is valid.

In summary, the observation of two-photon correlations has been successfully made for the first time in the X-ray region using a high-brilliance synchrotron radiation source. A unique method of obtaining $\gamma^{(2)}$ is developed, in which the total coincidence count, R , is normalized by the random coincidence count, R_0 , using a circulating electron bunch.

If a high-energy resolution sub-meV monochromator becomes available, a more remarkable correlation effect will be observed, and may possibly be applied to the following cases. This technique will be useful for characterization of the source size of third-generation synchrotron radiation sources just as Hanbury Brown & Twiss (1956*b*) determined the angular diameter of visible stars. Furthermore, in the study of X-ray laser action, the beam diagnosis concerning coherence at the transition from an incoherent state to a coherent state may be made.

We thank staff of the Tristan Super Light Facility and the Tristan Accelerator Department for construction and operation of the synchrotron radiation X-ray optics and the synchrotron radiation source. We also thank Mr E. Saito for his experimental support. This work was partially supported by a Grant-in-Aid for specially promoted research from the Ministry of Education, Science, Sports and Culture.

References

- Gluskin, E., McNulty, I., Vicario, P. J. & Howells, M. R. (1992). *Nucl. Instrum. Methods*, **A319**, 213–218.
- Goodman, J. W. (1985). *Statistical Optics*. New York: Wiley.

- Hanbury Brown, R. & Twiss, R. Q. (1956a). *Nature (London)*, **177**, 27–29.
- Hanbury Brown, R. & Twiss, R. Q. (1956b). *Nature (London)*, **178**, 1046–1048.
- Ikonen, E. (1992). *Phys. Rev. Lett.* **68**, 2759–2761.
- Shuryak, E. V. (1975). *Sov. Phys. JETP*, **40**, 30–31.
- Tanabe, T., Teich, M. C. & Marshall, T. C. (1991). *Nucl. Instrum. Methods*, **A304**, 77–80.
- Yamamoto, S., Sugiyama, H., Tsuchiya, K. & Shioya, T. (1997). *J. Synchrotron Rad.* **4**, 54–59.